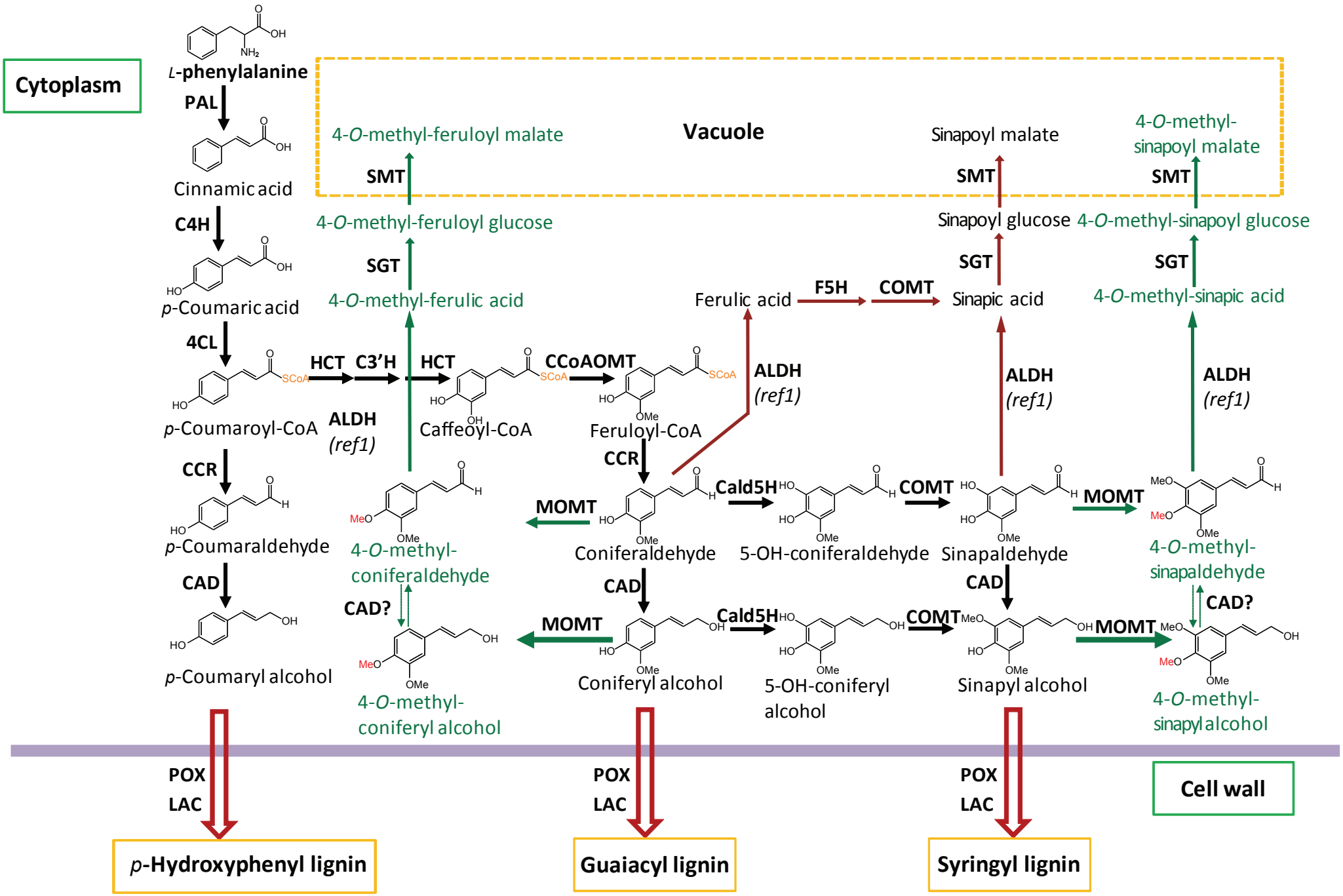

Supplemental Figure 1. The scheme of simplified phenylpropanoid-lignin-phenolic ester biosynthetic pathways

Arrows in black illustrate monolignol biosynthetic pathway. Arrows in magenta indicate the native sinapoyl malate pathway. Arrows in green indicate the putative pathways leading to the formation of novel phenolic esters after expression of MOMT. Dashed line arrows imply the putative steps.

PAL: phenylalanine ammonia lyase, C4H: Cinnamic acid 4-hydroxylase, 4CL: 4-Hydroxycinnamoyl CoA ligase, HCT: Hydroxycinnamoyl CoA: shikimate/quinate hydroxycinnamoyl-transferase, C3´H: *p*-Coumaroylshikimate 3´-hydroxylase, CCoAOMT: Caffeoyl CoA *O*-methyltransferase, CCR: Cinnamoyl CoA reductase, Cald5H/F5H: Coniferaldehyde/ferulate 5-hydroxylase, COMT: Caffeic acid/5-hydroxyferulic acid 3/5-*O*-methyltransferase, CAD: (Hydroxy)cinnamyl alcohol dehydrogenase, POX: Peroxidase, LAC: Laccase. ALDH: Aldehyde dehydrogenase, SGT: Sinapate glucosyltransferase, SMT: sinapoylglucose:malate sinapoyltransferase.

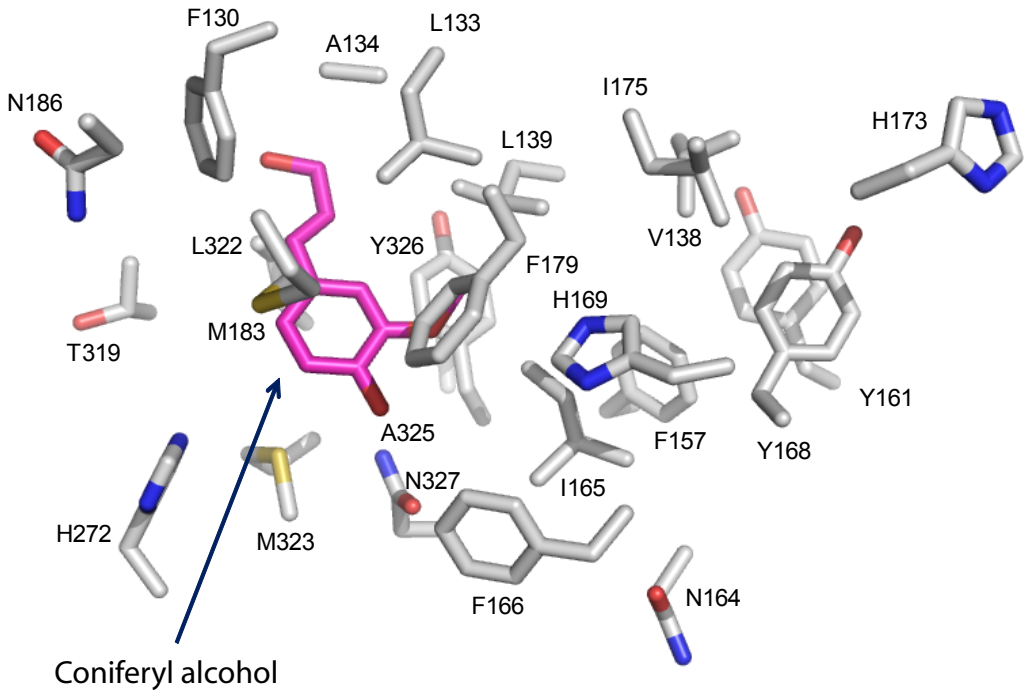

Supplemental Figure 2. Amino-acid residues directly in contact with, or proximate to the bound coniferyl alcohol in the MOMT3 active site.
The residues targeted for the iterative saturation mutagenesis were F130, A134, V138, L139, F157, Y161, N164, F166, Y168, H169, H173, F179, M183, N186, T319, L322, M323, A325, Y326, and N327.

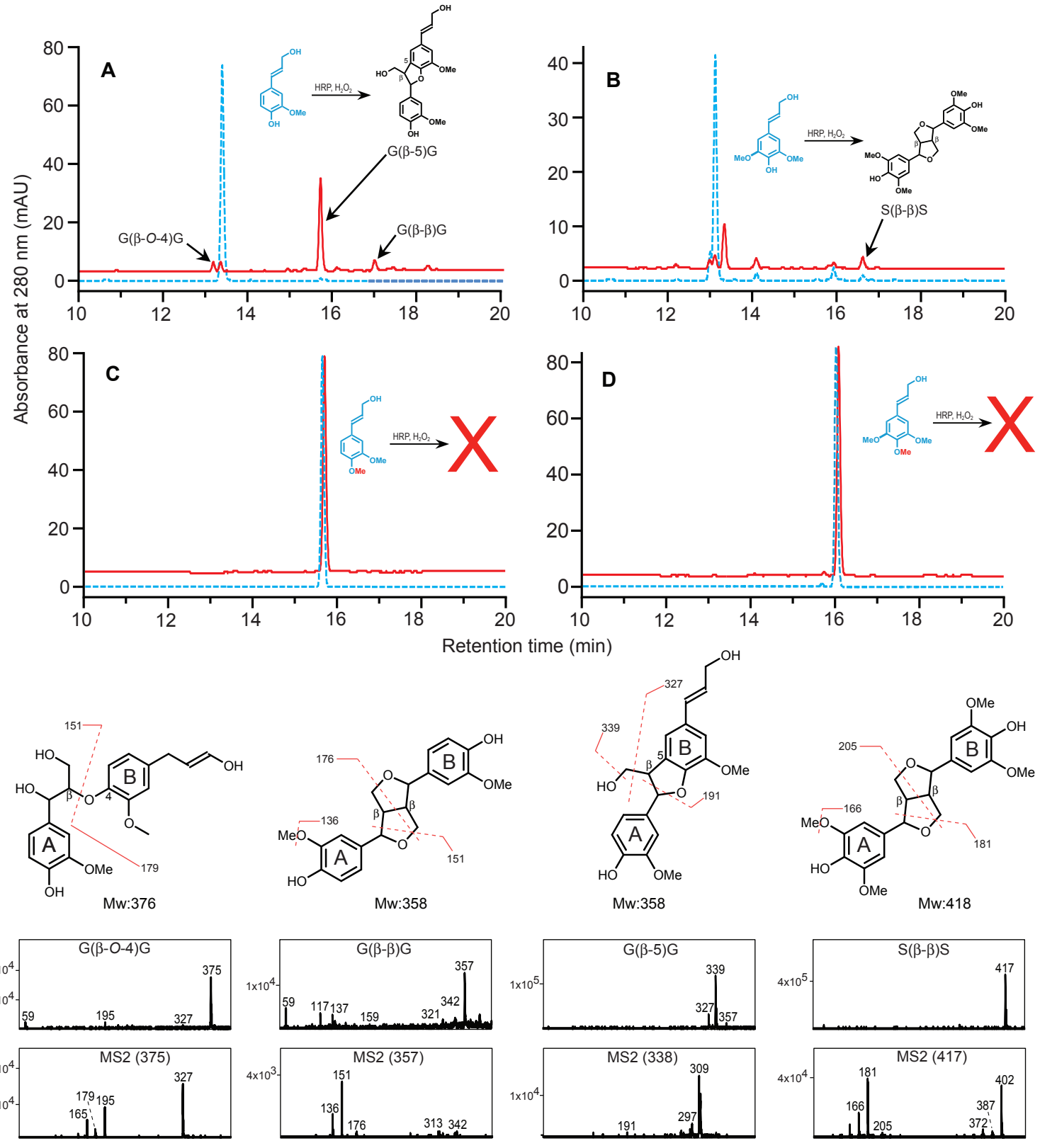

Supplemental Figure 3. *In vitro* **polymerization of conventional monolignols and 4-*O*-methylated monolignols.**
(**A**) LC-MS profile of the reaction of coniferyl alcohol incubated with horseradish peroxidase and H2O2 (solid line), or with buffer alone as the control (dashed line). The profile shows a predominant dimer G(β–5)G and the minor products of G(β–*O*–4)G and G(β–β)G. The corresponding ESI-mass spectra of the dimeric products are shown.
(**B**) LC-MS profile of the reaction of sinapyl alcohol incubated with horseradish peroxidase and H2O2 (solid line), or with buffer alone as the control (dashed line). The profile identifies a dimer S(β–β)S. Its tandem ESI-mass spectra are shown.
(**C**) LC-MS profile of the reaction of 4-*O*-methyl-coniferyl alcohol incubated with horseradish peroxidase and H2O2 (solid line), or with buffer alone (dashed line). As expected, no dimers or oligomers were detected.
(**D**) LC-MS profile of the reaction of 4-*O*-methyl-sinapyl alcohol incubated with horseradish peroxidase and H2O2 (solid line), or with buffer alone (dashed line). As expected, no dimers or oligomers were detected.

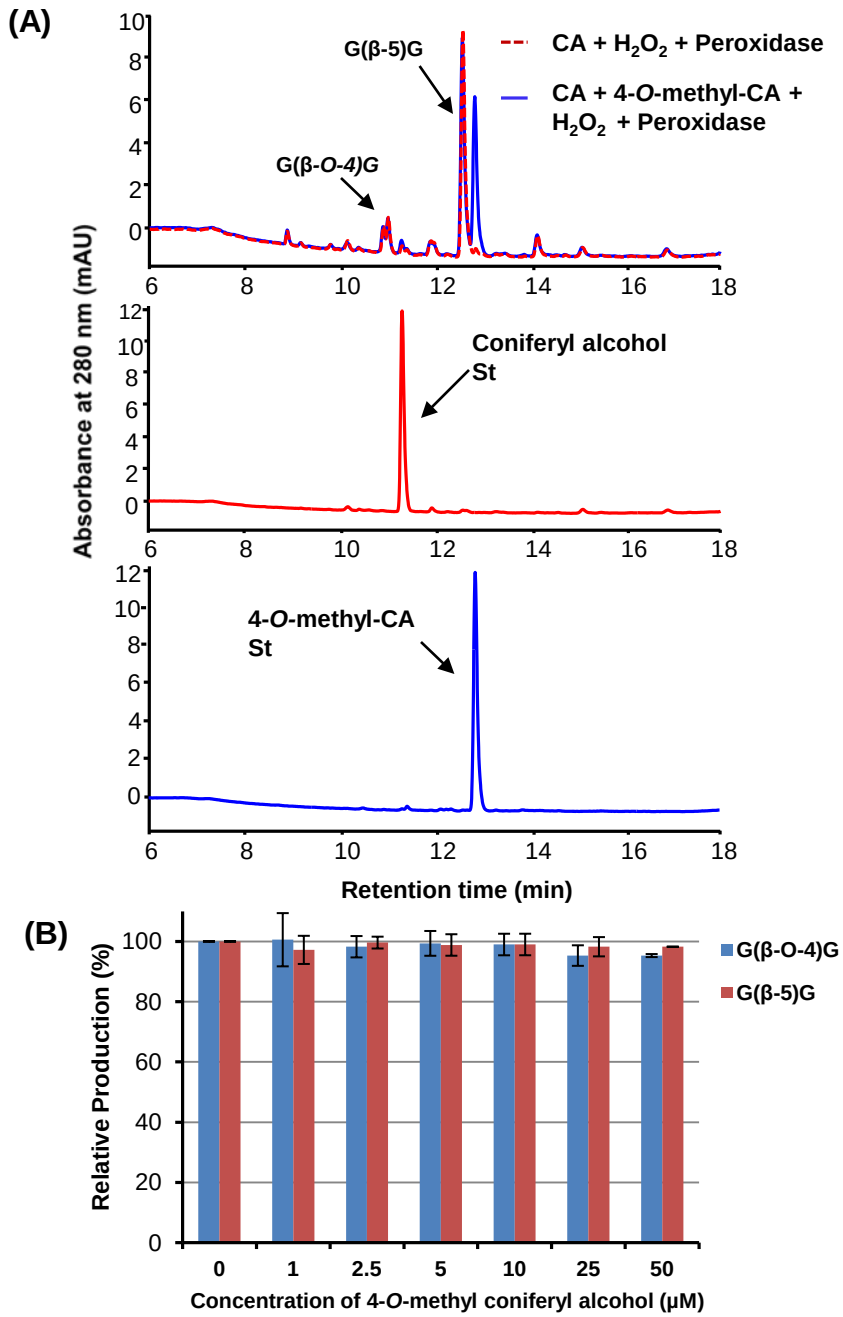

Supplemental Figure 4. Co-incubation of Conventional Monolignol with 4-*O*-Methylated Monolignol in the *In Vitro* Polymerization System.

(A) HPLC profiles of the reactions incubating coniferyl alcohol alone (red line), or both coniferyl alcohol and 4-*O*-methyl-coniferyl alcohol (blue line) with horseradish peroxidase and H_2O_2. No difference was discernible in the production of oligomers from the two sets of reactions. CA: coniferyl alcohol.

(B) Examination of potential inhibition of 4-*O*-methyl-coniferyl alcohol on oxidative coupling of coniferyl alcohol. The production of major dimers G(β–5)G and G(β–*O*–4)G was quantified and compared to that in the reaction of coniferyl alcohol alone (which was set as 100%). The data are the mean and SD of two replicates.

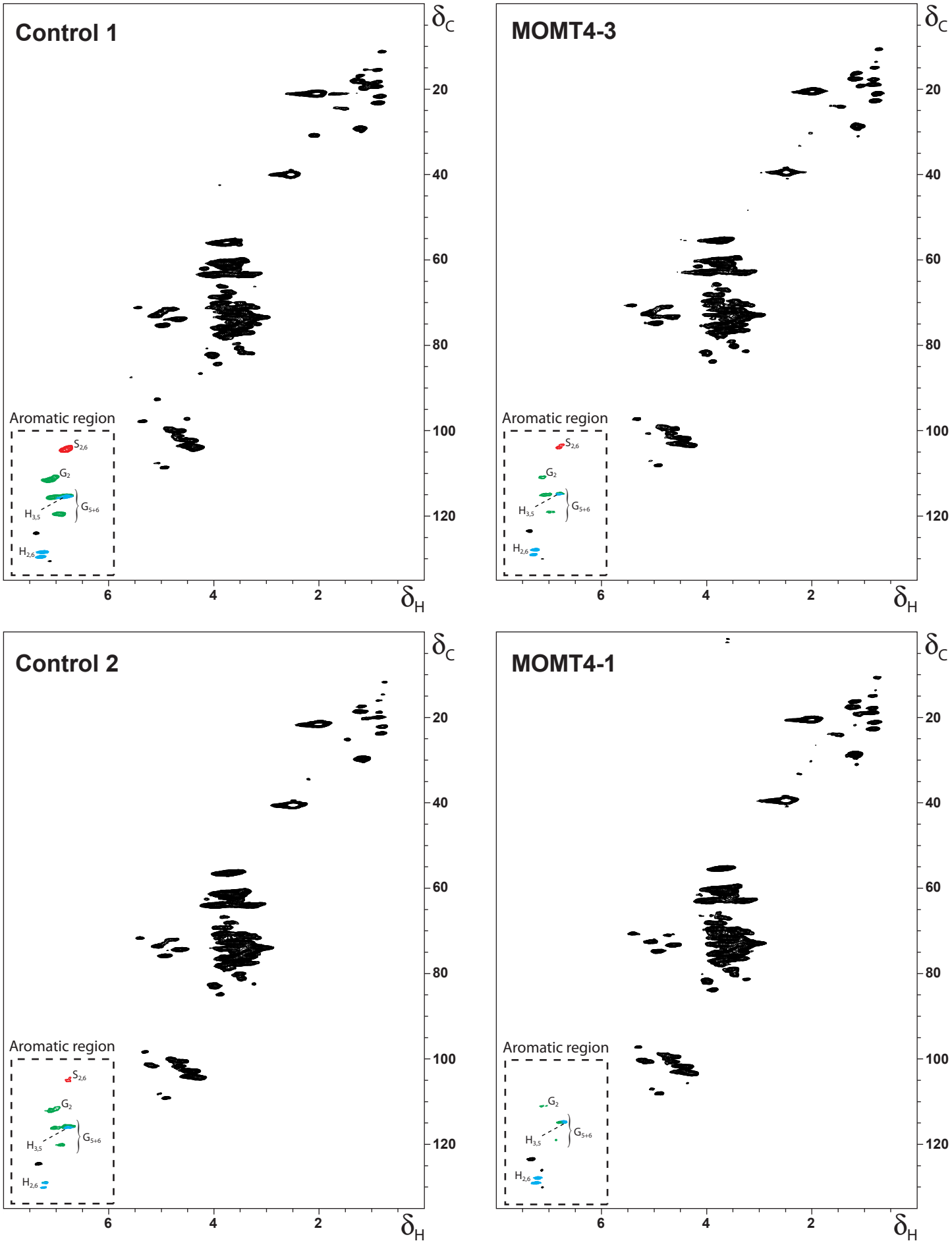

Supplemental Figure 5. HSQC NMR spectra (δC/δH 0-135/0-8.0 ppm) of the cell walls of MOMT4 transgenic and control lines after forming a gel in DMSO-d6:pyridine-d5 (4:1).

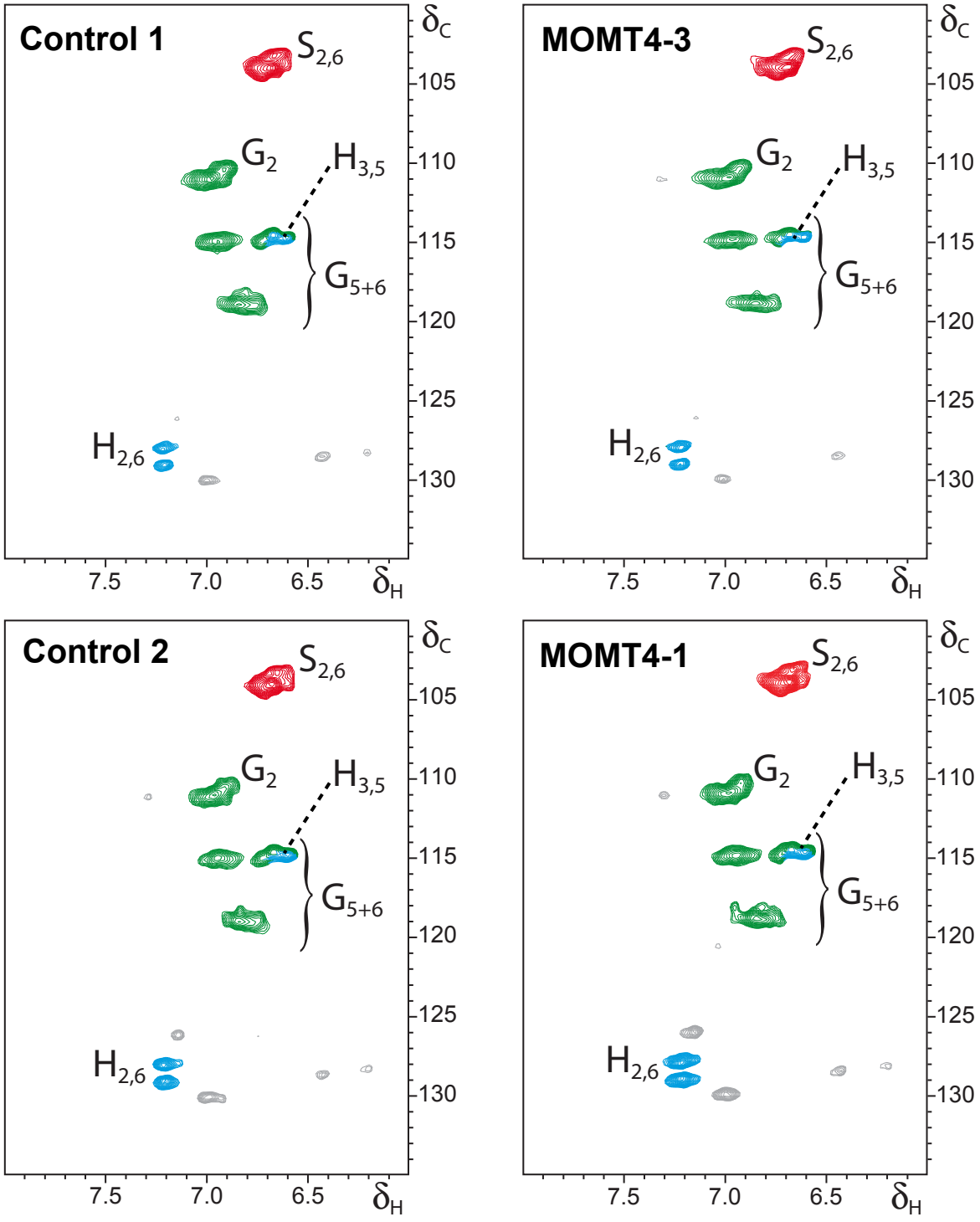

Supplemental Figure 6. Partial short-range 13C-1H(HSQC) spectra (aromatic regions) of CELs isolated from the cellwalls of two control and MOMT transgenic lines.

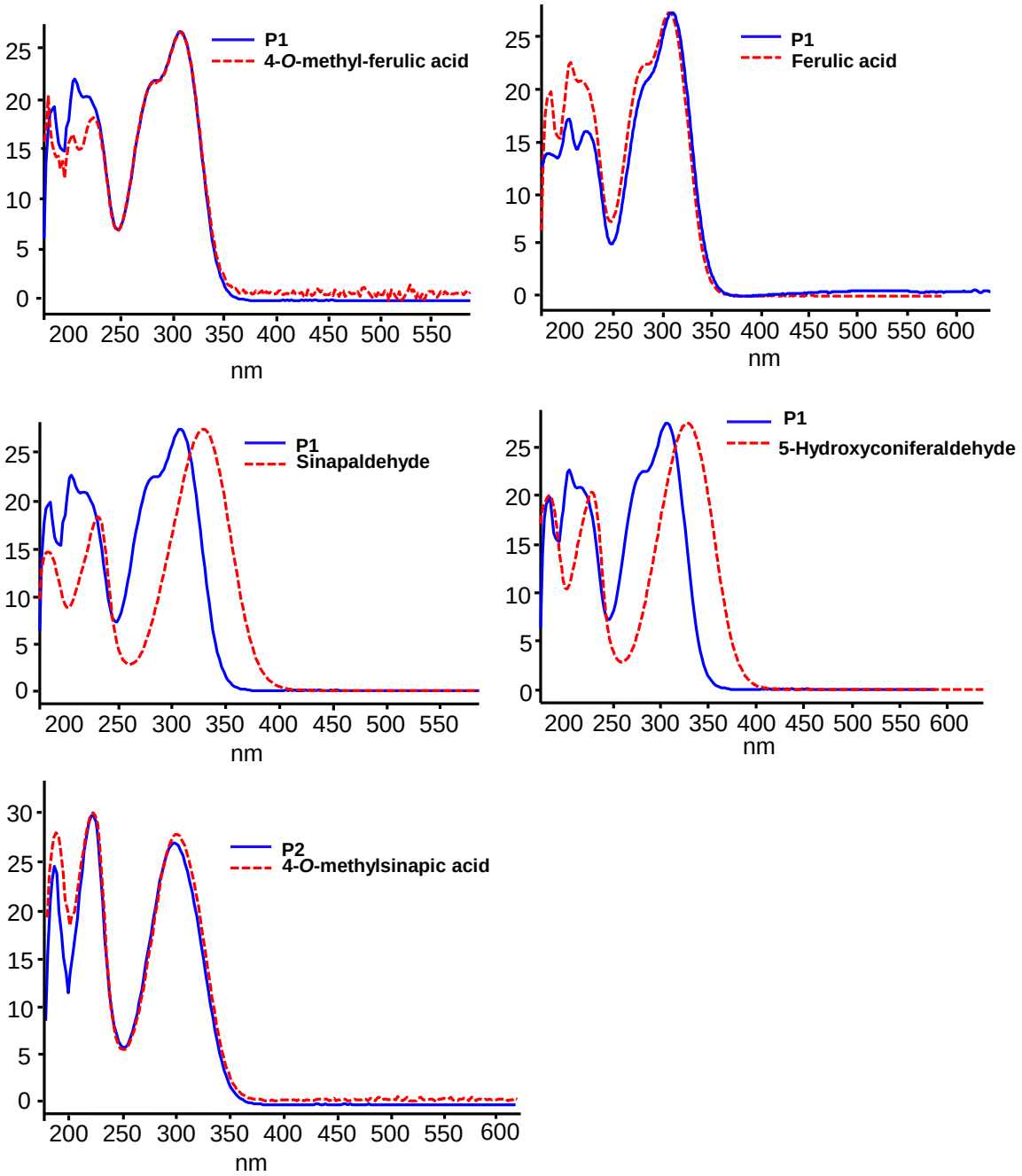

Supplemental Figure 7. The UV Spectra of Novel "Wall-Bound" Phenolic Esters and the Related Phenolic Standards.

The spectrum of P1 in Figure 6 is identical to that of the enzymatic product 4-*O*-methyl-ferulic acid and similar to its parental compound ferulic acid, but differs from those aldehyde analogues; similarly the spectrum of P2 is identical to that of enzymatic product 4-*O*-methyl-sinapic acid.

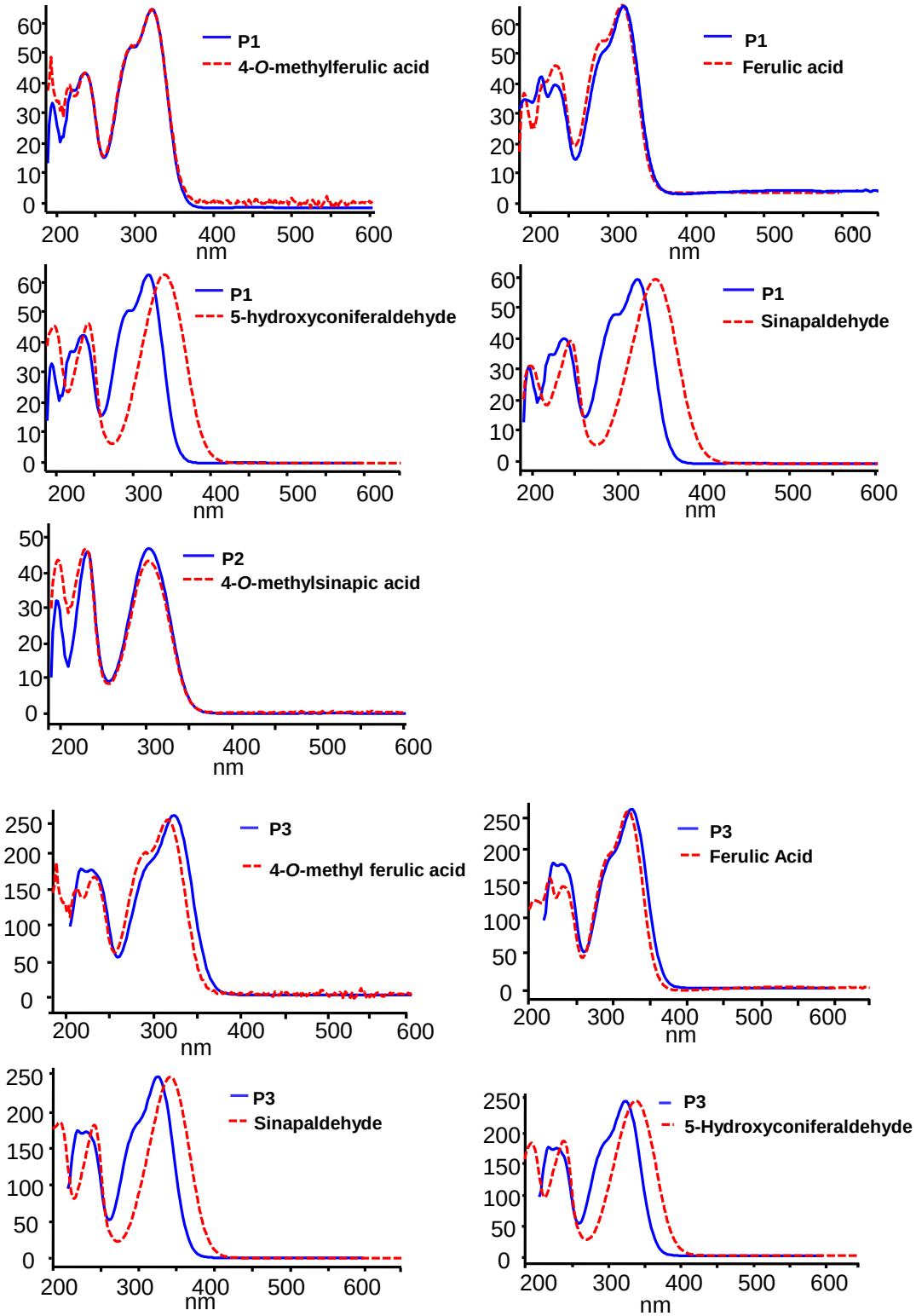

Supplemental Figure 8. The UV Spectra of Novel Soluble Phenolic Esters and the Related Phenolic Standards.

The spectrum of P1 and P3 in Figure 7 is similar to those of the enzymatic product 4-*O*-methyl-ferulic acid and its parental compound ferulic acid, but differs from those of aldehyde analogues; the spectrum of P2 is similar to that of enzymatic product 4-*O*-methyl-sinapic acid.

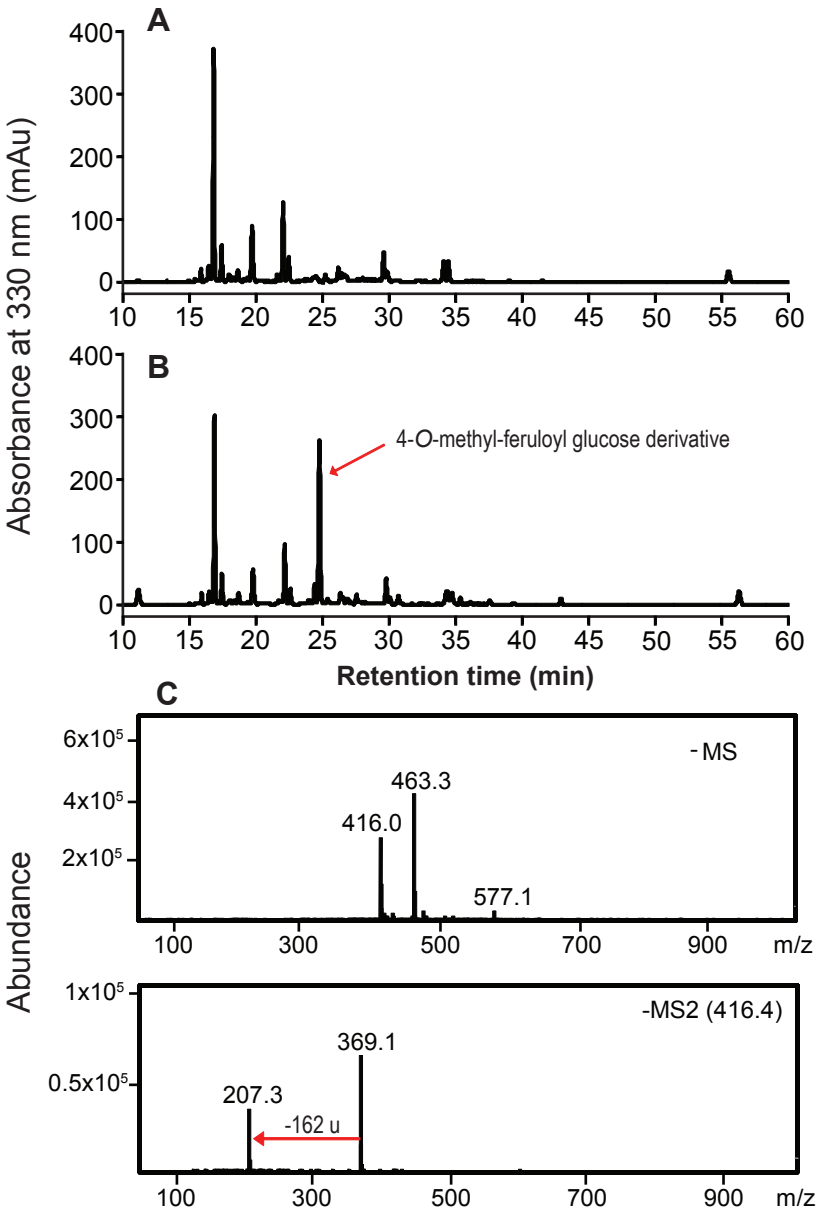

Supplemtal Figure 9. LC-MS analysis on novel methanolic soluble-phenolic compounds accumulated in the root of MOMT4 transgenic plants.

(**A**) HPLC profiles of phenolic extract from roots of control plants, and (**B**) MOMT4 transgenic plants. The major novel compound accumulated in MOMT4 expression plant is the 4-*O*-methyl-feruloyl glucose derivative; its corresponding MS spectra are shown in (**C**).

Supplemental Table 1. The Kinetic parameters of MOMT variants for monolignols.

Protein	K_m (μM)	V_{max} (nmol. mg $^{-1}$.min $^{-1}$)	K_{cat}/K_m (M^{-1} s^{-1})
Coniferyl alcohol			
IEMT wild type	1591 ± 182	42 ± 3.5	17.6
T13M-E165F	546.4 ± 62.2	352.7 ± 19.2	430.3
T133L-E165F	279.9 ± 18.3	117 ± 2.9	278.6
T133L-E165I-F175I	279.2 ± 48.2	556.2 ± 35.6	1327.9
T133L-E165I-F175I-Y161W	196.3 ± 33.6	583.8 ± 36.9	1986.1
T133L-E165I-F175I-Y161F	196.5 ± 21.2	642.2 ± 24.2	2172.2
T133L-E165I-F175I-F166W	117.6 ± 15	496.6 ± 8.2	2825.7
T133L-E165I-F175I-H169F	192.6 ± 24.5	793 ± 32.4	2738.7
T133L-E165I-F175I-H169M	219.7 ± 27	629 ± 26.2	1905.7
T133L-E165I-F175I-A325V	235.9 ± 49.8	446.2 ± 32.7	1259.7
T133L-E165I-F175I-F166W-H169W	127.2 ± 8.1	392.1 ± 9.4	2054.7
T133L-E165I-F175I-F166W-T135N	166.9 ±10.9	431.3± 11.7	1722.5
T133L-E165I-F175I-Y326F-N327V	143.5 ± 12.8	474.5 ± 12.4	2204
Sinapyl alcohol			
IEMT wild type	1495 ± 214.4	44.6 ± 3.9	19.9
T13M-E165F	326 ± 59.5	84.7 ± 6.2	173.2
T133L-E165F	381.9 ± 32.3	102.7 ± 3.7	179.2
T133L-E165I-F175I	119.6 ± 15.5	274.7 ± 9.5	1527.5
T133L-E165I-F175I-Y161W	218.7 ± 19.1	259.1 ± 7.6	788.3
T133L-E165I-F175I-Y161F	205.6 ± 25	289.2 ± 12.3	937.6
T133L-E165I-F175I-F166W	47.1 ± 8.6	146.6 ± 5.3	2084.7
T133L-E165I-F175I-H169F	68.1 ± 11.1	407.5 ± 16.5	3999.3
T133L-E165I-F175I-H169M	88.9 ± 10.4	369.7 ± 11.0	2771.1
T133L-E165I-F175I-A325V	96.9 ± 6.9	214 ± 3.8	1470.5
T133L-E165I-F175I-F166W-H169W	67.6 ± 12.9	160.5 ± 11.9	1582.6
T133L-E165I-F175I-F166W-T135N	54.5 ± 14.2	115 ± 8.6	1406.5
T133L-E165I-F175I-Y326F-N327V	298.3 ± 29.2	301 ± 11.2	672.6

The data represent the mean ± S.E. of two replicates.

Supplemental Table 2. Crystallographic data sheet for MOMT3-coniferyl alcohol-SAH structure

Data collection	
Space group	$P2_1$
Cell dimensions	
a, b, c (Å)	65.86, 152.16, 68.18
α, β, γ (˚)	90.00, 94.92, 90.00
Resolution range (Å)[a]	50-2.4 (2.47-2.40)
Observations	291,566
Unique reflections	52,117
Completeness (%)[a]	100 (99.9)
Redundancy[a]	5.6 (5.1)
I/σ[a]	26.1 (2.0)
R_{sym} (%)[a,b]	13.0 (50.4)
Refinement	
R_{cryst}/R_{free} (%)[c]	19.3 (26.1)
No. of atoms	
Protein	10743
Water molecules	166
SAH	104
Phenolic substrate	52
RMSD	
Bonds (Å)	0.008
Angles (˚)	1.4
Average B factors	
Protein (Å^2)	20.8
water (Å^2)	19.1
SAH (Å^2)	18.7
Phenolic substrate (Å^2)	80.6

[a] Number is parentheses refer to the highest shell.
[b] Rsym = $|I_h - \langle I_h \rangle|/I_h$, where $\langle I_h \rangle|$ is the average intensity over symmetry equivalent reflections.
[c] $R_{cryst} = \sum|F_{obs} - F_{calc}|/ \sum F_{obs}$, where summation is over the data used for refinement, R_{free} was calculated using 5% of data excluded from refinement.

Supplemental Table 3. Quantification of soluble phenolics in ten-week-old stems of MOMT4 transgenic plants [a]

Phenolics	Control	MOMT-1	MOMT-2	MOMT-3	MOMT-4
4-*O*-methyl-feruloyl malate[b]	ND	619.6 ± 21	411 ± 26.1	770.5 ± 53.7	384.6 ± 57
4-*O*-methyl-sinapoyl malate	ND	153 ± 4.6	127.3 ± 6.4	316.5 ± 10.1	192.8 ± 11
4-*O*-methyl-feruloyl glucose	ND	57.8 ± 1.7	17.2 ± 2.8	41.8 ± 8.3	13.8 ± 2.7
Sinapoyl malate	ND	ND	ND	ND	ND
Feruloyl malate	ND	ND	ND	ND	ND
Kaempferol 3-*O*-[6"-*O*-(rhamnosyl) glucoside]-7-*O*-rhamnoside	204.7 ± 66.2	269.5 ± 52.1	147 ± 30.6	301.5 ± 38.2	180.3 ± 32.7
Kaempferol 3-*O*-rhamnoside-7-*O*-glucoside	268.2 ± 45	231.1 ± 57.2	112.4 ± 27.5	251.8 ± 32.7	150.7 ± 31.3
Kaempferol 3-*O*-rhamnoside 7-*O*-rhamnoside	608.3 ± 112.1	551.6 ± 84.4	330.2 ± 53	617.1 ± 62.5	368 ± 53.7

[a] The data represent the means and standard errors from four or five analyses (n≥4).

[b]The quantity of the soluble compounds are expressed in nanomole per gram fresh weight stems

ND, Not detectable